의학석사 학위논문

Effects of a new generation of AIMP1-derived peptide (AdP) on wound healing

AIMP1 유래 펩타이드의 상처 치료 효과 규명

2022년 8월

서울대학교 대학원

의학과 성형외과학 전공

장신뤼

Effects of a new generation of AIMP1-derived peptide (AdP) on wound healing

지도 교수 허찬영

이 논문을 의학석사 학위논문으로 제출함
2022년 4월

서울대학교 대학원
의학과 성형외과학 전공
장신뤼

장신뤼의 의학석사 학위논문을 인준함
2022년 7월

위 원 장 김상화 (인)

부위원장 허찬영 (인)

위 원 나정임 (인)

Abstract

Effects of a new generation of AIMP1-derived peptide (AdP) on wound healing

ZHANG XINRUI

Department of Plastic and Reconstruction Surgery

College of Medicine

The Graduate School

Seoul National University

The skin plays an important role in protecting the body from mechanical damage, microbial infection, ultraviolet radiation, and extreme temperatures. Many products as well as ongoing studies have focused on skin injury and repair; however, unlimited challenges are still being faced. Furthermore, the drugs that are currently on the market are not adequate to meet the increasing medical needs. This study aimed to discover whether our new product can efficiently promote wound repair and skin restoration. In this study, we applied a new aminoacyl tRNA synthetase complex interacting 1-derived peptide (AdP), NeoPep S, administered in two dose types (1ppm and 3ppm), and determined their effect on skin wound repair in rat models. Cell proliferation and inflammatory responses were assessed using immunofluorescence (IF) staining and enzyme-linked immunosorbent assay (ELISA). Our results showed more rapid and satisfactory progress in wound closure upon treatment with NeoPep S 3ppm than with NeoPep S 1ppm. The 3ppm

peptide derived from aminoacyl tRNA synthetase complex interacting multifunctional protein 1 (AIMP1), harmoniously interacted with the wound to promote re-epithelialization and collagen regeneration, as well as the down-regulation of several types of cytokines and chemokines, such as tumor necrosis factor alpha (TNF-α), interleukin 6 (IL-6), interleukin 8 (IL-8), interleukin 1 beta (IL-1β), monocyte chemoattractant protein 1 (MCP-1), and F4/80. Moreover, it was demonstrated to promote fibroblast proliferation, migration, and differentiation by transforming growth factor beta 1 (TGF-β1) and transforming growth factor beta 3 (TGF-β3) modulation, as well as nitrite and reactive oxygen species, scavenging. In short, the novel peptide NeoPep S 3ppm has high effectiveness and safety in wound healing and shows great promise in becoming one of the leading wound care products in the near future.

Keywords : Wound healing, peptide, aminoacyl tRNA synthetase complex interacting 1 (AIMP1), collagen, extracellular matrix

Student Number : 2020-26237

Table of Contents

List of Figures

Introduction

The skin is not only the largest organ of the human body and the most important protective barrier against external environmental agents, but it also has many other essential roles, such as temperature regulation, metabolism, absorption, reception, and secretion, as well as immunity. Therefore, the consistency of the skin structure in ensuring the complete performance of all the functions is crucial. However, skin can be affected by irregular external factors, such as mechanical, thermal, chemical, and radiative factors, leading to damage and imbalance, or serious structural effects on function (1, 2). Following these injuries, the human body generally initiates a multi-stage wound repair and healing process that includes: hemostasis, inflammation, proliferation, and remodeling. Many variables, including cell types such as keratinocytes, fibroblasts, macrophages, platelets, and endothelial cells, as well as cell-derived mediators, such as vascular endothelial growth factor (VEGF), transforming growth factor-beta (TGF-β), interleukin (IL), and platelet-derived growth factor (PDGF), tightly control and coordinate each stage (3, 4).

Despite the fact that skin regeneration is a natural process, a variety of conditions may interfere with the phases of healing, producing extensive healing or chronic wounds. Pathogens can more easily infiltrate and harm chronic wounds, resulting in inflammation, septicemia, electrolyte and water imbalances, multi-organ damage, and secondary diseases, as well as increasing the psychological burden and financial economy of patients (5). The formation of scar tissue and keloids are common side effects of extensive wound healing that can influence the aspect, function, and esthetics of the skin (6). Both chronic wounds and extensive healing have an impact on the biological mechanisms of the skin, resulting in the creation of more significant health problems, as well as increased clinical treatment charges (7-9).

Many efforts have been made to identify effective procedures for wound healing treatments. Although there are many new technologies that have been applied that are attractive, including stem cells and tissue engineering, other therapies are still urgently being researched (4, 10-12). Nowadays, the most common medical drugs consist of small molecules and grown factors. However, these single-type drugs have many disadvantages, including being unstable carriers and being difficult to synthesize; carrying out unsatisfactory activities; needing to be stored under strict situations; being easily rendered inactive through storage or transport; and, most importantly, their use may result in intemperate wound repair, giving rise to hypertrophic scars (13-15). Nevertheless, wound repair and skin restoration still face unlimited challenges, and the current drugs on the market are inadequate to meet the increasing medical needs. Therefore, finding and developing new medications with high activity and low production costs is important.

In the last five years, 15 peptide molecules and peptide derivatives drugs have been approved by the U.S. Food Drug Administration (FDA) with many great successes, such as AfamelanotideScenesse®, Semaglutide Ozempic®, Bremelanotide Vyleesi®, and AbaloparatideTymlos®, accounting for 7% of the total number of drugs (208 new drugs) and 25.8% of the biological drugs (16, 17). These peptide drugs indicate many advantages worth considering, including straightforward compound discoveries, high affinity and specificity for receptors *in vivo*, ideally high reliability, limited toxic metabolism, rapid approval rate, low levels of accumulation, and fewer medication interchanges (18, 19). However, among these achievements, very few non-growth factor peptides have emerged to have the capability to improve the skin wound repair process (20). Thus, wound healing peptides with increased activity, high stability, and low cost are still needed in the market.

Aminoacyl tRNA synthetase complex interacting multifunctional

protein 1 (AIMP1) is a prominent protein with many applications in medications. The drugs developed from aminoacyl tRNA synthetase complex interacting multifunctional protein 1 (AIMP1) and its derivatives have been demonstrated for use in therapies for systemic lupus erythematosus, alopecia, and rheumatoid arthritis (21-23). Moreover, Aminoacyl tRNA synthetase complex interacting multifunctional protein 1 (AIMP1) has been modified under peptide variants, i.e., so-called aminoacyl tRNA synthetase complex interacting 1-derived peptide (AdP). In addition, the impacts of the derivatives of the protein on skin cells have opened up many possibilities for cutaneous studies. For example, the potential of aminoacyl tRNA synthetase complex interacting 1-derived peptide (AdP) (amino acid region 6-46) in skin repair was shown through extracellular signal-regulated kinase (ERK) activation, resulting in fibroblast proliferation and collagen generation that improved wound healing (24, 25). In the cosmeceutical field, aminoacyl tRNA synthetase complex interacting 1-derived peptide (AdP) was applied as an ingredient in an anti-aging and whitening cosmetic product (26, 27). Nevertheless, the potential of aminoacyl tRNA synthetase complex interacting 1-derived peptide (AdP) in skin wound repair has not yet been discovered. In this study, we applied a new generation of aminoacyl tRNA synthetase complex interacting 1-derived peptide (AdP), NeoPep S cream, containing a short peptide chain with a length of 15 amino acids, and carried out *in vivo* experiments to examine the contribution as well as the effect of NeoPep S on the wound healing process. The experiments were performed using hematoxylin and eosin (H&E) staining, Masson's trichrome (MT) staining, immunofluorescence (IF) staining, and enzyme-linked immunosorbent assay (ELISA). The results from NeoPep S showed great efficacy, including promotion of the wound healing process and inhibition of inflammatory cytokines, indicating that it could be a promising drug for the treatment of wounds.

Materials and Methods

Materials and reagents

Fetal bovine serum (FBS) (#16000044) and Dulbecco's Modified Eagle Medium (DMEM) (#11965118) were purchased from Gibco (Grand Island, NY, USA). Nitrite and Griess reagent (modified) were ordered from Sigma Aldrich (St. Louis, MO, USA). PRO-PREP Protein Extraction Solution (#17081) was from iNtRON(Seongnam, Gyeonggi, Republic of Korea). The Pierce™ BCA Protein Assay Kit (#23225) was from Thermo Fisher Scientific (Waltham, MA, USA. Tissue Extraction Reagent I was ordered from Invitrogen (Carlsbad, CA, USA). Mouse monoclonal IgG1 κ vimentin antibody (sc-6260), smooth muscle actin antibody (sc-53015), and F4/80 antibody (sc-377009) were purchased from Santa Cruz Biotechnology (Dallas, TX, USA). Purified hamster anti-mouse/rat TNF (cat: 557516), purified mouse anti-rat MCP-1 (cat: 555072), and purified mouse anti-rat IL6 (cat: 550644) were obtained from BD PharmingenTM(San Diego, CA, USA). Rat IL-1 beta (cat: MAB501) and rat IL-8 antibodies were purchased from R&D Systems (MN, Canada). Rabbit anti-mouse IgG (H+L) Cross-Adsorbed Secondary Antibody Alexa Fluor 488 (#A-11059) was from Invitrogen (Carlsbad, CA, USA). Elisa kits (TNF-α, IL8, and IL-1β) were obtained from MyBioSource (San Diego, CA, USA). The nitrocellulose membrane was a product of Bio-Rad (Hercules, CA, USA). Anti-TGF beta 1 antibody was from Abcam (1:100, #ab92486; Cambridge, MA, USA).

Peptide preparation and examination

The NeoPep S peptide with high purity (>95%) used in this research was synthesized and prepared by CG Bio Co., Ltd (Seoul, Republic of Korea). A new variant of AIMP1-derived peptide composed of 15 amino acids, 1,700 Da, was generated. The original substance was formed under white powder, then creamed in distilled

water with neither color nor fragrance. The creams, at a mass of 1ppm and 3ppm, were tested and then used to treat wound areas after surgery.

Cell viability and cytotoxicity

NIH-3T3 cells (4×10^4 well/cell) were grown in 96-well plates overnight. The cells were then treated and incubated with 0.5, 5, and 50 μg/ml of NeoPep S for 24, 48, and 72 h. The viability of the cells was analyzed using the MTT assay. In brief, the cells were incubated with media containing 0.5 mg/ml MTT at 37 ℃, 5% CO_2 for 4 h. Subsequently, all media were removed and rinsed with 1×phosphate buffered saline (PBS). The formazan product was dissolved in 100 μl of dimethyl sulfoxide. The absorbance at 570 nm was then measured. The viability of the non-treated cells and the cells treated with NeoPep S were evaluated.

Evaluation of NeoPep S with lipopolysaccharide

RAW 264.7 cells (2.5×10^5 cells/well) in 24-well plates were cultured at 37 ℃, 5% CO_2 overnight. Next, concentrations of lipopolysaccharide (LPS) at 500 ng/ml were co-incubated with or without NeoPep S at 0.5, 5, and 50 μg/ml at 37 ℃, 5% CO_2 for 3 h. The supernatants were collected and stored at −80 ℃ for further experiments.

Evaluation of intracellular nitrite and nitrate production

Inflammation of RAW 264.7 cells was conducted using 500 ng/ml lipopolysaccharide (LPS) with and without NeoPep S (0.5, 5, and 50 μg/ml) co-incubated for 3 h at 37 ℃, 5% CO_2. Next, 100 μl of the inflamed media supernatant was mixed with 100 μl of 1X Griess modified reagent. The mixed solution was incubated at room

temperature for 15 min. Subsequently, measurements of nitric oxide were determined by carrying out a microplate reader of the absorbance at 540 nm.

Evaluation of intracellular reactive oxygen species level

RAW 264.7 cells (12×10^4 cells/well)in 96-well plates were grown and incubated at 37 ℃ , 5% CO_2 overnight. Subsequently, concentrations of lipopolysaccharide (LPS) at 500 ng/ml were co-incubated with or without NeoPep S at 0.5, 5, and 50 μg/ml at 37 ℃, 5% CO_2 for 3 h. All media were removed and washed with 1× PBS buffer. The cells were washed with 1× phosphate buffered saline (PBS), 20 μM of DCF-DA solution was added, and incubation occurred at 37 ℃, 5% CO_2 for 45 min in the dark. The fluorescence was measured using a microplate reader at 485 and 535 nm excitation and emission, respectively.

In vivo wound healing experiment

For the *in vivo* wound experiment, we used 8-week-old Sprague Dawley rats (BioOrient Company, Republic of Korea) weighing 250–300g that were grown for 12/12h in a light/dark cycle and maintained in pathogen-free conditions with free access to food and drinking water. The animal experiments were authorized by the Institutional Animal Care and Use Committee of Seoul National University Bundang Hospital (approval number: BA-1802-241-014-08), and all the methods followed the NIH Guidelines for the Care and Use of Laboratory Animals. Ten rats from each group were wounded and then treated with NeoPep S creams at 1ppm and 3ppm doses separately. The animals were first anesthetized with isoflurane (Hana Pharm, Republic of Korea), the dorsum was shaved, and their skin was then cleaned with 70% alcohol and betadine. A 10-mm-diameter round wound was made by a puncture on the skin in the mid-dorsal

region. The wounds were treated with creams and covered with a light dressing. The cream treatments were repeated once a day for 10 days. We monitored the wound healing progress daily and calculated the wound sizes. Moreover, five rats per group were chosen randomly and biopsied on days 7 and 10, respectively. The 12-mm-diameter circle area of the wound tissue for biopsy consisted of the epidermis and dermis.

Wound size measurement

The kinetics of the wound closures from all samples was captured using digital photography on days 0, 3, 7, and 10 after removing all wound dressings. The wound sizes were then measured and calculated using ImageJ software (version 1.53e, National Institute of Health, Bethesda, MD, USA). The following equation was used to calculate the percentage of wound healing:

$$\text{Percentage of wound healing} = (A0 - An)/ A0 \times 100\%$$

where A0 represents the original wound size immediately after surgery, and An indicates the wound size on day n after surgery. The rats in each group were analyzed on the same day to evaluate the approximate levels of wound closure.

Hematoxylin and eosin staining

The tissue sections underwent deparaffinization in xylene for 30 min before being rehydrated in different declining concentrations of ethanol (100%, 95%, and 80%), and were then washed with distilled water every 5 min. To reduce background staining, after 5 min in hematoxylin, the samples were rinsed for 3 min in phosphate buffered saline (PBS). The samples were then stained for 2 min with eosin, rinsed for 5 min with distilled water, and then dehydrated every 5 min in 80%, 90%, and 100% ethanol, followed by 15 min in

xylene. Finally, the slides were mounted with neutral resin and coverslipped. A light microscope (Zeiss Axio Scope.A1, Carl Zeiss, Göttingen, Germany) was used to examine the stained sections and to capture photographs. The thickness of the epidermis was measured using ImageJ software, and statistical analysis was performed.

Masson's trichrome staining

Following the manufacturer's indicated techniques, the tissue sections were performed through deparaffinization and rehydration and then stained using a Masson's trichrome staining kit. Briefly, the cell nuclei were stained for 5 min with A1:A2 (1:1), and then thoroughly rinsed with water and soaked in acid alcohol for 3 s to differentiate. The fibrous tissues were stained for 5 min with a Ponceau acid fuchsin solution, and then followed with a series of 1 min with 2% acetic solution, 30 s with phosphomolybdic for differentiation, and 20 s with aniline blue before being dehydrated, mounted, and coverslipped, as described above. Masson's trichrome stained tissues were used to assess collagen fiber synthesis and intensity by using ImageJ software.

Immunofluorescence staining

The tissue sections underwent deparaffinization and hydration, followed by the blocking of the non-specific binding sites by dropping 4% bovine serum albumin (BSA) in phosphate buffered saline (PBS) at room temperature for 1 h. The blocked sections were then incubated with a mouse monoclonal IgG1 κ vimentin antibody (1:100, sc-6260, Santa Cruz Biotechnology) diluted in 4% bovine serum albumin (BSA) in phosphate buffered saline (PBS) overnight at 4 ℃. After washing with phosphate buffered saline (PBS), a rabbit anti-mouse IgG Alexa Flour 488®-conjugated secondary antibody (1:1,000, # A-11059, Invitrogen) was prepared and incubated for the sections in the dark for 1 h at room temperature, followed by nuclear

labeling with DAPI and mounting with antifade mounting medium. Imaging of the fluorescent signals was then performed using a confocal microscope (Zeiss LSM 710 or LSM 800, ZEN software, Germany). The images were then analyzed for vimentin intensity using ImageJ software.

Enzyme-linked immunosorbent assay

The tissue sections from the wound area were obtained from the rats on days 7 and 10 post-surgery and then immersed in liquid nitrogen to snap freeze. The samples were next homogenized in PROPREPTM Protein Extraction Solution (C/T) (#17081, iNtRON, Republic of Korea) following the manufacturer's suggested protocol. After the last step of centrifugation at 14,000 ×g for 15 min at 4℃, the supernatants were collected and the expression levels of tumor necrosis factor alpha (TNF-α), interleukin 1 beta (IL-1β), Interleukin 6 (IL-6), monocyte chemoattractant protein 1 (MCP-1), and Interleukin 8 (IL-8) cytokines in the wound tissues were determined using enzyme-linked immunosorbent assay (ELISA) kits (MyBioSource, CA, USA) following the manufacturer's instruction accordingly.

Determination of nitrite and nitrate production by nitric oxide assay

A nitric oxide assay was used for the quantitative determination of nitrite and nitrate in the wound tissue lysates using the Griess modified reagent. The wound sections were collected on day 7 and day 10, and protein was extracted as described above. The extracts were cleared by centrifugation at 14,000 rpm for 15 min at 4℃, and then the supernatants were collected and diluted 1:1 with distilled water. A mix of 100 μl of 1X Griess modified reagent and 100 μl of diluted protein extract was incubated at room temperature for 15 min. The absorbance was measured at the wavelength 540 nm. The nitrite

standard solution was prepared for dilution with ranges from 0 to 50 μM.

Determination of ROS level from tissue protein by DCF-DA assay

The wound sections were collected on days 7 and 10, and protein was extracted as described above. The extracts were cleared by centrifugation at 14,000 rpm for 15 min at 4 ℃, and then the supernatants were collected. Next, 20 μM of DCF-DA solution was added and incubation occurred at 37℃, 5% CO_2 for 45 min in the dark. The fluorescent signals were read at 485 and 535 nm excitation and emission, respectively.

Statistical analysis

All information was gathered through measurements and provided as mean ± standard error of the mean (SEM). Statistical analysis was carried out using GraphPad Prism 8 (GraphPad Software Inc., San Diego, CA, USA), and the differences between the groups were established using an unpaired two-tailed t-test. To be considered statistically significant, we required a p-value < 0.05 (95% confidence interval) for three to five independent experiments.

Results

Cell viability and the evaluation of cytotoxicity

NIH-3T3 cells were cultured in various concentrations of NeoPep S to compare the cytotoxicity activities. The 24-hour result depicts that all the different concentrations of NeoPep S slightly reduced the cell viability. However, the 48-hour result demonstrated the cell viability of the 0.5 μg/ml of NeoPep S group was higher than the other groups while that of 50 μg/ml of NeoPep S group was the lowest. After 72-hour treatment, the viability of Raw cells was almost the same among different groups. The differences in cell viability among distinct groups were always less than 10% throughout the time period. Altogether, the usage of NeoPep S does not affect cell viability.

Figure 1

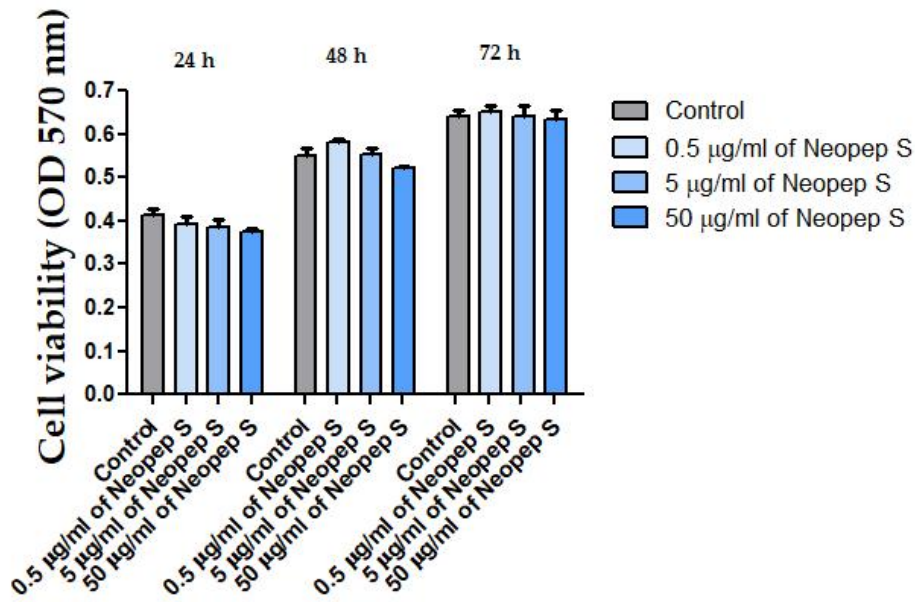
Cell viability (OD 570 nm)
24 h
48 h
72 h
0.0
0.1
0.2
0.3
0.4
0.5
0.6
0.7
Control
0.5 μg/ml of Neopep S
5 μg/ml of Neopep S
50 μg/ml of Neopep S

Figure 1. Results of cell viability and the evaluation of cytotoxicity. Cell viability of NIH-3T3 cells among four different groups (named Control, 0.5 μg/ml of Neopep S, 5 μg/ml of Neopep S, and 50 μg/ml of Neopep S) after 24 hours, 48 hours, and 72 hours respectively.

The effect of NeoPep S on RAW 264.7 cells

The effect of NeoPep S on LPS-induced inflammatory cytokine production was quantified by using RAW 264.7 cells. RAW 264.7 cells were co-treated with 0.5, 5, and 50 μg/ml of NeoPep S, and 500 ng/ml of LPS for 3 h. The level of inflammatory cytokines, such as tumor necrosis factor alpha (TNF-α), interleukin 1 beta (IL-1β), interleukin 6 (IL-6), and monocyte chemoattractant protein 1 (MCP-1), in the supernatant of the media, was determined using the enzyme-linked immunosorbent assay (ELISA) method. As shown in Figure 2A, the concentration of tumor necrosis factor alpha (TNF-α) in the lipopolysaccharide (LPS)-stimulated RAW 264.7 cells showed a more than ten-fold increase compared with that in the control group. However, the level of tumor necrosis factor alpha (TNF-α) production reduced with the NeoPep S treatment. In particular, 50μ/ml of NeoPep S significantly inhibited tumor necrosis factor alpha (TNF-α) production in the lipopolysaccharide (LPS)-stimulated RAW 264.7 cells. The concentration of tumor necrosis factor alpha (TNF-α) decreased by over 70% compared with that in the lipopolysaccharide (LPS) group.

Similar results were exhibited for other inflammatory cytokines, such as interleukin 6 (IL-6), interleukin 1 beta (IL-1β), and monocyte chemoattractant protein 1 (MCP-1) (Figure 2B-D). The concentration of inflammatory cytokines surged by a large margin in the lipopolysaccharide (LPS) group compared with the control group, showing that lipopolysaccharide (LPS) can give rise to the secretion of inflammatory cytokines. However, the concentration of inflammatory cytokines declined to relatively low degrees with an increasing concentration of NeoPep S treatment. In short, this finding revealed that NeoPep S can inhibit the secretion of inflammatory cytokines and play a significant role in relieving inflammation. This function contributes to wounds recovering quickly during the wound healing process.

Moreover, the effect of NeoPep S on nitric oxide production in the culture supernatant of the inflamed RAW 264.7 cells was examined using a nitric oxide (NO) assay method. As shown in Figure 2E, nitric oxide (NO) production was significantly increased in the lipopolysaccharide (LPS)-treated RAW 264.7 cell group compared with the control group. The amount of nitric oxide (NO) production in the inflamed RAW 264.7 cells treated with different concentrations of NeoPep S showed meaningful declines, ranging between 72.79% and 87.56%.

Apart from that, the effect of NeoPep S was confirmed by detecting the reactive oxygen species (ROS) level in the RAW 264.7 cells. As demonstrated in Figure 2F, the lipopolysaccharide (LPS)-induced 264.7 cells produced a reactive oxygen species (ROS) level that was two-fold higher than that in the control group. Meanwhile, the levels of reactive oxygen species (ROS) production in the NeoPep S treatment groups were significantly decreased compared with those in the lipopolysaccharide (LPS) treatment group. At a high concentration of NeoPep S, there was a considerably reduced reactive oxygen species (ROS) level in the lipopolysaccharide (LPS)-stimulated RAW 264.7 cells.

Figure 2

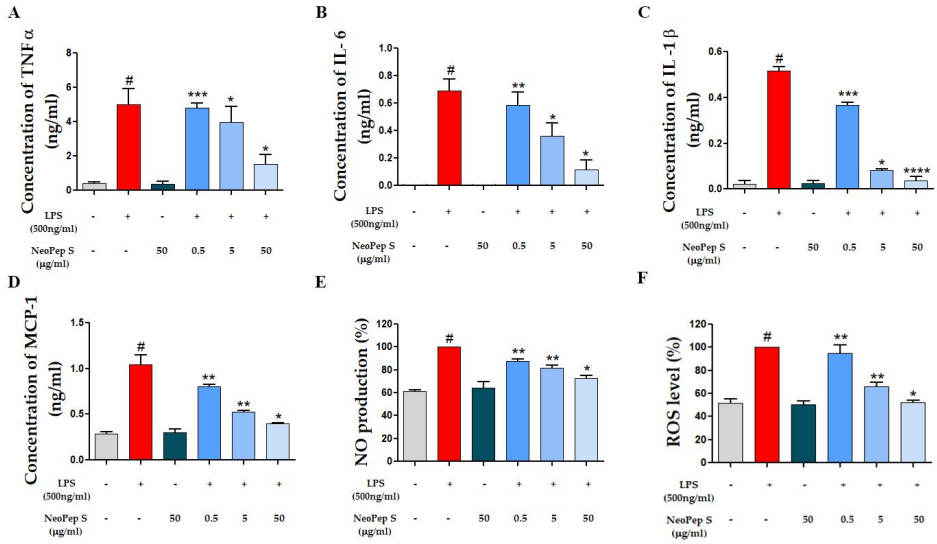
A
Concentration of TNF α (ng/ml)
B
Concentration of IL- 6 (ng/ml)
C
Concentration of IL -1β (ng/ml)
D
Concentration of MCP-1 (ng/ml)
E
NO production (%)
F
ROS level (%)
LPS (500ng/ml)
NeoPep S (μg/ml)
- + - + + +
- - 50 0.5 5 50

Figure 2. The results of cell culture. (A-D) The results of the enzyme-linked immunosorbent assay (ELISA) for the RAW cells showed increases in the secretion of pro-inflammatory cytokines after the application of lipopolysaccharide (LPS), and a down-regulation of the expression of tumor necrosis factor alpha (TNF-α), interleukin 1 beta (IL-1 β), interleukin 6 (IL-6), and monocyte chemoattractant protein 1 (MCP-1) after using various concentrations of NeoPep S. (E, F) Comparison of reactive oxygen species (ROS) level and nitric oxide (NO) production among different groups.

The effect of NeoPep S on wound healing *in vivo*

The NeoPep S 1ppm and 3 ppm were applied to wounds every day to investigate *in vivo* wound healing. All the rats survived and in time showed gradual wound healing without infection. The wound healing process was photographed on days 0, 3, 7, and 10, and the percentage of wound healing was then measured. In the NeoPep S 1ppm and 3 ppm groups, the wound healing size showed faster wound closure than for the control group each time. As shown in Figure 3A–C, the wound healing size was 67.88% in the control group after 3 days, whereas the wound healing sizes in the NeoPep S 1ppm and 3ppm groups were 48.75% and 42.97%, respectively, for the same period. On day 7 post-wounding, application of the NeoPep S 1ppm and 3ppm resulted in 16.39% and 12.20% wound closure, respectively, whereas only 25.33% wound closure was observed in the control group. The wounds treated with NeoPep S 1ppm and 3ppm were completely healed with 3.62% and 2.76% wound closure, respectively, by day 10, while 10.56% of the wound closure remained unhealed in the control group. The quantification of the wound healing size revealed that the NeoPep S 3ppm group had the highest percentage of wound closure, which was considerably different from that of the control group.

In order to further evaluate the wound healing, a histological analysis was conducted using hematoxylin and eosin (H&E) staining to determine the restoration level of the epidermis layer. Figure 3D presents the hematoxylin and eosin (H&E) staining pictures of all the groups on day 7 and day 10. It is clear from the results that 7 days after surgery, there was already epidermis formation in all groups. The thickness of the re-epithelialized tissue in each group was measured based on hematoxylin and eosin (H&E) staining. On day 7, the average thickness of the re-epithelialized tissue in the NeoPep S 3ppm group was the highest, followed by that in the NeoPep S 1ppm and control groups, respectively. The results of day 10 showed a similar trend after a certain increase. The thickness of the re-

epithelialized tissue in the NeoPep S 3ppm and NeoPep S 1ppm groups were both higher than that of the control group (61.80 ± 3.92 μm), at 73.01 ± 3.59 μm and 80.5 ± 5.33μm, respectively. A histological evaluation of the wound sections observed a decrease in wound width for the NeoPep S groups compared with the control group on days 7 and 10 of wound healing (Figure 3E). In addition, on days 7 and 10, a histological examination of the hematoxylin and eosin (H&E)-stained wound sections demonstrated a reduction in wound width for the NeoPep S 1ppm and 3 ppm treatment groups, compared with the control group. The wound width and thickness of the re-epithelialized tissue in the NeoPep S 3ppm group were consistently the highest among all groups during the whole wound healing process.

Collagen production and deposition are also important for wound healing. As shown in Figure 3F, Masson's trichrome (MT) staining revealed that the collagen fibers were relatively spare and disordered in the untreated group, while those in the NeoPep S 1ppm and 3 ppm groups were bundled on day 7. On day 10, the intensity of the collagen fibers in the NeoPep S 1ppm (37.04%) and NeoPep S 3ppm (39.55%) groups was significantly denser compared with those in the control group (28.68%) (Figure 3G). We can conclude from this result that the treated wounds in the NeoPep S groups (especially the NeoPep S 3 ppm group) had a higher collagen content than the control group. Taken together, these results show that NeoPep S 3ppm accelerates wound healing by promoting inflammation in the early stages as well as collagen synthesis.

Figure 3

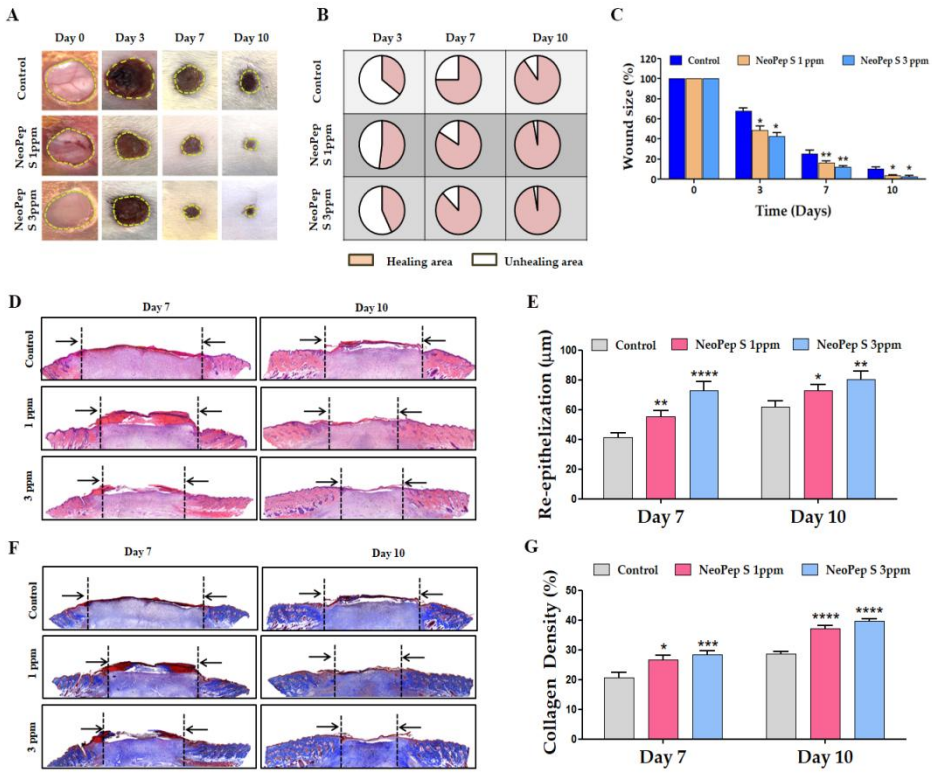
A
Day 0
Day 3
Day 7
Day 10
Control
NeoPep S 1ppm
NeoPep S 3ppm
B
Day 3
Day 7
Day 10
Control
NeoPep S 1ppm
NeoPep S 3ppm
Healing area
Unhealing area
C
Control
NeoPep S 1 ppm
NeoPep S 3 ppm
Wound size (%)
Time (Days)
D
Day 7
Day 10
Control
1 ppm
3 ppm
E
Control
NeoPep S 1ppm
NeoPep S 3ppm
Re-epithelization (μm)
Day 7
Day 10
F
Day 7
Day 10
Control
1 ppm
3 ppm
G
Control
NeoPep S 1ppm
NeoPep S 3ppm
Collagen Density (%)
Day 7
Day 10

Figure 3. NeoPep S promoted the wound healing process, re-epithelialization, and collagen deposition. (A) Wound healing was analyzed post-surgery. Wound closure photos were captured from the control, NeoPep S 1 ppm, and NeoPep S 3 ppm on days 0, 3, 7, and 10 post-surgery by macroscopic photography. (B) Schematic diagram of the healing process of all groups by wound sizes. The circle represents the entire wound, while the sections in skin color and white color indicate the healing and unhealing areas, respectively. (C) Quantification analysis of wound size on days 0, 3, 7, and 10 show that NeoPep S promoted the wound healing process *in vivo*. (D) Hematoxylin and eosin (H&E) staining images of the wound groups on day 7 and day 10. (E) The re-epithelialization thickness of each group on day 7 and day 10. (F) Masson's trichrome (MT) staining images of all groups on day 7 and day 10. (G) Collagen density of various groups on day 7 and day 10. Statistical differences were performed using an unpaired two-tailed t-test. ****$p<0.0001$, ***$p<0.001$, **$p<0.01$, and *$p<0.05$ compared with the control group.

NeoPep S promoted the proliferation of fibroblasts

To evaluate the effect of NeoPep S 1ppm and NeoPep 3ppm on wound healing, the collected tissues from days 7 and 10 were stained with vimentin, which acts as an integrator of the wound healing processes, controlling fibroblast proliferation and the epithelial-mesenchymal transition (EMT)-like transdifferentiation of keratinocytes, both of which are critical for successful wound repair using the immunofluorescence (IF) staining method. As Figure 4A&B shows, the intensity of vimentin significantly increased in both NeoPep S groups compared with the control group over time. On day 7, the vimentin intensity was highest in the NeoPep S 3ppm group (68.71 ± 2.12), while it was 64.97 ± 1.92 and 45.44 ± 2.4 in the NeoPep S 1ppm group and the control group, respectively. The same trend was observed on day 10. The NeoPep S 3ppm group still released the highest vimentin intensity at 78.86 ± 7.17, followed by the NeoPep S 1ppm group at 70.21 ± 2.24, while the vimentin intensity in the control group was the lowest at 51.71 ± 2.70 (Figure 4C).

Figure 4

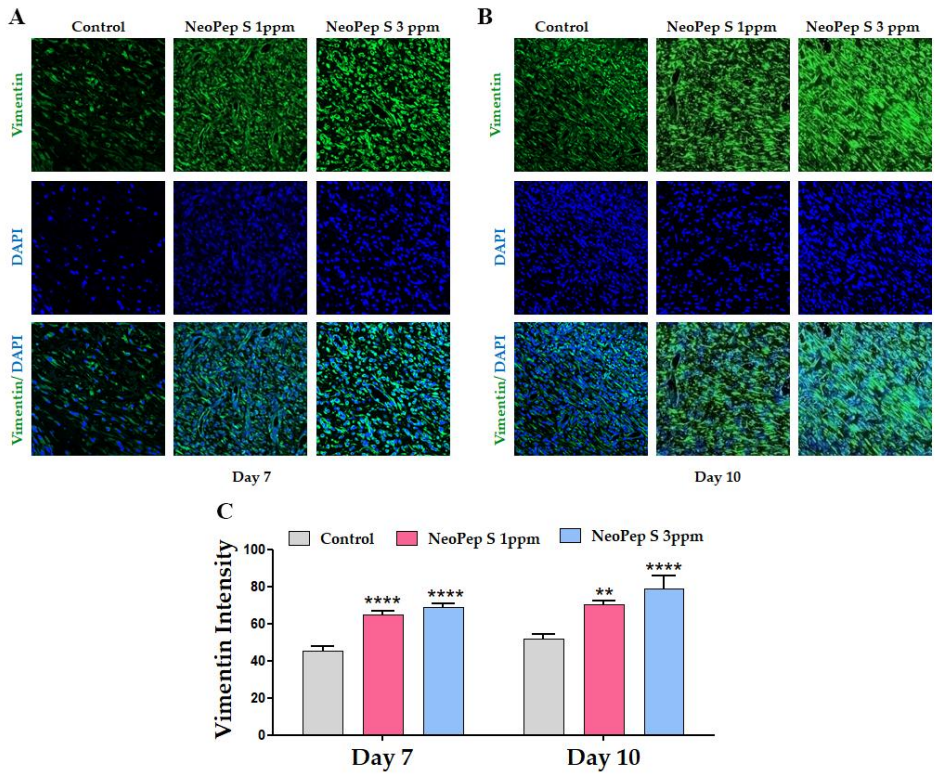
A
Control
NeoPep S 1ppm
NeoPep S 3 ppm
Vimentin
DAPI
Vimentin/ DAPI
Day 7
B
Control
NeoPep S 1ppm
NeoPep S 3 ppm
Vimentin
DAPI
Vimentin/ DAPI
Day 10
C
Control
NeoPep S 1ppm
NeoPep S 3ppm
Vimentin Intensity
100
80
60
40
20
0
****
****
**
****
Day 7
Day 10

Figure 4. The effect of NeoPepS on the proliferation of fibroblasts. Green fluorescence indicates a positive signal of vimentin expression, accordingly. Blue illustrates nuclear 4′,6-diamidino-2-phenylindole (DAPI) staining. The scale bar represents 20 μm. (A) Immunofluorescence (IF) staining images of each group on day 7. (B) Immunofluorescence (IF) staining images of each group on day 10. (C) Comparison of immunofluorescence (IF) intensity for each group. ****$p<0.0001$, ***$p<0.001$, **$p<0.01$, and *$p<0.05$.

NeoPep S led to the down-regulation of pro-inflammatory cytokines in the wound

To quantify the remaining inflammatory cytokines during the wound healing processes, tissues from days 7 and 10 were stained with inflammatory cytokine biomarkers, such as interleukin 1 beta (IL-1β) and interleukin 6 (IL-6), using the immunofluorescence (IF) staining method. Regarding the interleukin 1 beta (IL-1β) biomarker, a key mediator of the inflammatory response, a significant reduction in intensity was revealed in the NeoPep S 3ppm group-treated wound sites on day 7 at 55.05 ± 3.59, whereas it was at 65.37 ± 3.29 and 97.05 ± 4.64 for the NeoPep S 1ppm and control groups, respectively for the same period. On day 10 post-wounding, the intensity of interleukin 1 beta (IL-1β) in the NeoPep S 3ppm group was the lowest at 44.39 ± 2.16, followed by the NeoPep S 1ppm group at 53.54 ± 2.89, and only 80.62 ± 5.99 interleukin 1 beta (IL-1β) intensity was observed in the control group (Figure 5A-C).

In addition, interleukin 6 (IL-6), a key modulator marker of inflammatory cytokine, was also examined using the IF staining method. The results showed there was a significant down-regulation of the cytokine profile during the examination time, indicating a sharp reduction in inflammation. The interleukin 6 (IL-6) intensity was relatively high in the control group (71.27 ± 4.35) but was significantly decreased in the NeoPep S 1ppm group (42.38 ± 2.25) and NeoPep S 3ppm group (38.58 ± 2.16). Similarly, on day 10, the NeoPep S 3ppm group showed the lowest IL-6 intensity at 32.50 ± 1.52, whereas 38.76 ± 2.25 and 57.21 ± 3.97 were observed in the NeoPep S 1ppm and control groups, respectively (Figure 6A-C).

Figure 5

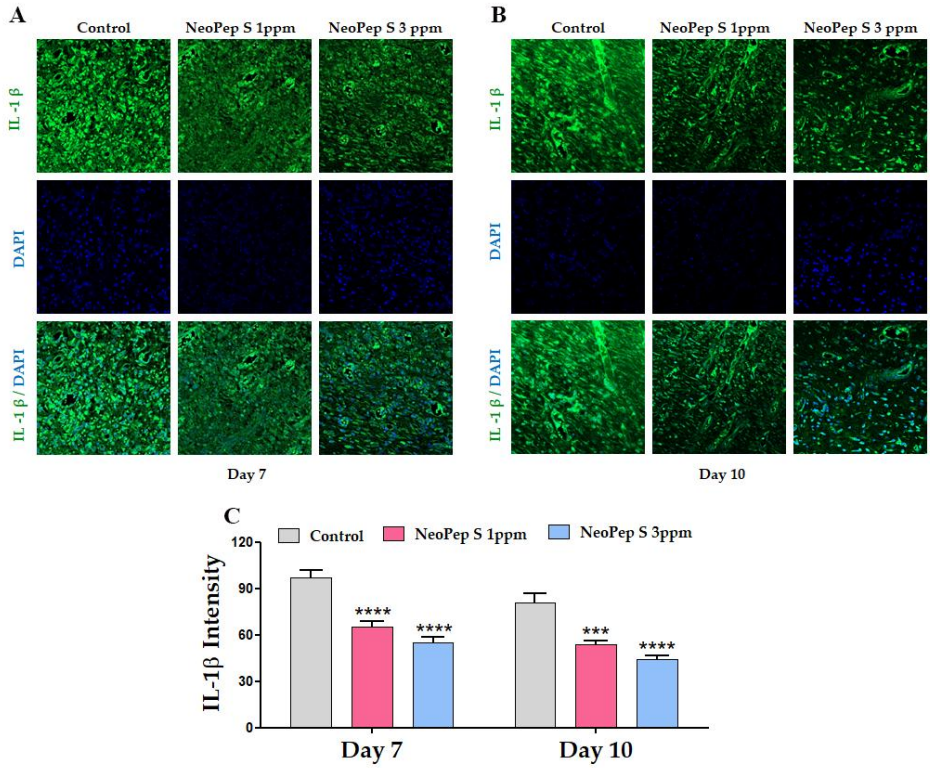
A
Control
NeoPep S 1ppm
NeoPep S 3 ppm
IL-1β
DAPI
IL-1β / DAPI
Day 7
B
Control
NeoPep S 1ppm
NeoPep S 3 ppm
IL-1β
DAPI
IL-1β / DAPI
Day 10
C
Control
NeoPep S 1ppm
NeoPep S 3ppm
IL-1β Intensity
120
90
60
30
0
****
****
***
****
Day 7
Day 10

Figure 5. The effect of NeoPep S on anti-inflammation. Green fluorescence indicates a positive signal of interleukin 1 beta (IL-1β) expression, accordingly. Blue illustrates nuclear 4′,6-diamidino-2-phenylindole (DAPI) staining. The scale bar represents 20 μm. (A) Immunofluorescence (IF) staining images of each group on day 7. (B) Immunofluorescence (IF) staining images of each group on day 10. (C) Comparison of immunofluorescence (IF) intensity for each group. ****$p<0.0001$, ***$p<0.001$, **$p<0.01$, and *$p<0.05$.

Figure 6

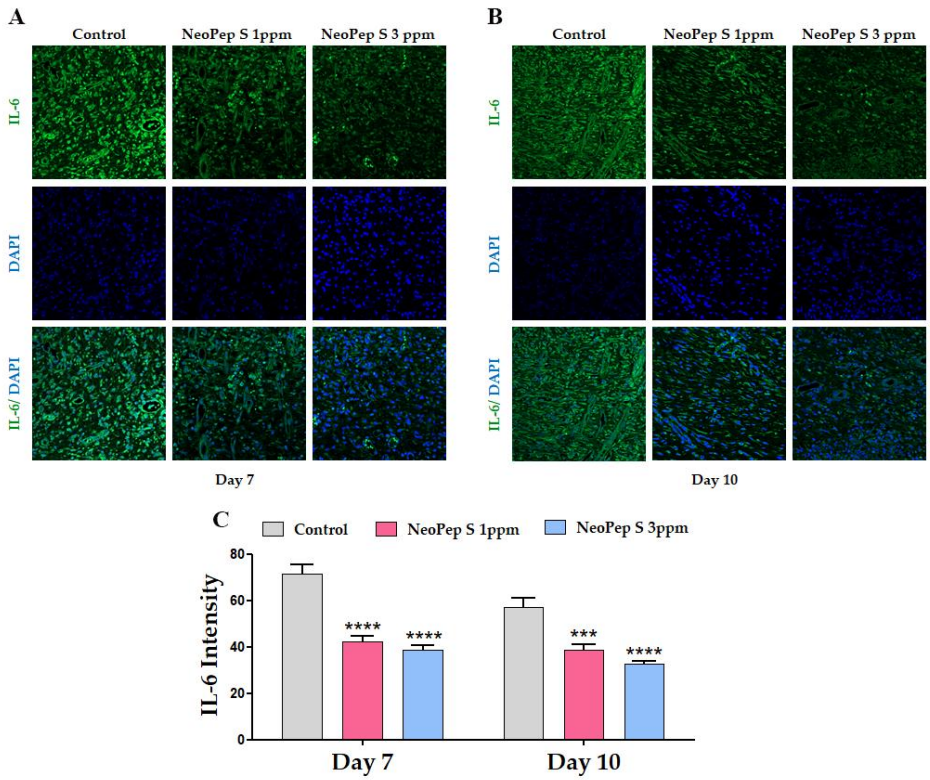
A
Control
NeoPep S 1ppm
NeoPep S 3 ppm
IL-6
DAPI
IL-6/ DAPI
Day 7
B
Control
NeoPep S 1ppm
NeoPep S 3 ppm
IL-6
DAPI
IL-6/ DAPI
Day 10
C
Control
NeoPep S 1ppm
NeoPep S 3ppm
IL-6 Intensity
80
60
40
20
0
****
****
***
****
Day 7
Day 10

Figure 6. Inflammatory cytokines/chemokines in various stages of wound healing with NeoPep S peptide treatment. Green fluorescence indicates a positive signal of interleukin 6 (IL-6) expression, accordingly. Blue illustrates nuclear 4′,6-diamidino-2-phenylindole (DAPI) staining. The scale bar represents 20 μm. (A) Immunofluorescence staining images of each group on day 7. (B) Immunofluorescence staining images of each group on day 10. (C) Comparison of immunofluorescence (IF) intensity for each group. ****$p<0.0001$, ***$p<0.001$, **$p<0.01$, and *$p<0.05$.

The effect of NeoPep S on cytokine expression, nitric oxide production, and reactive oxygen species level *in vivo*

To measure the expression of cytokines in the wound healing tissues, proteins were purified from collected skin tissues on day 7 and day 10 using a protein extraction kit. Cytokine expression was quantified by ELISA assay. The concentration of interleukin 1 beta (IL-1β) in the NeoPep S groups was observed as lower than that in the control group over time. The concentrations of interleukin 1 beta (IL-1β) in the NeoPep S 1ppm (26.01± 2.82 pg/mg, p=0.037) and NeoPep S 3ppm (21.05± 1.94 pg/mg, p=0.034) groups at day 7 were lower compared with those in the control group (41.50± 5.78 pg/mg). In addition, at day 10, the concentration of IL-1β in the NeoPep S 3ppm group was the lowest (13.62 ± 1.07 pg/mg, p=0.034) compared with those in the NeoPep S 1ppm (14.78 ± 0.75 pg/mg, p=0.028) and control groups (18.8 ± 1.3 pg/mg), respectively (Figure 7A). Furthermore, Figure 7B-E shows a similar trend for interleukin (IL-6), monocyte chemoattractant protein 1 (MCP-1), tumor necrosis factor alpha (TNF-α), and interleukin 8 (IL-8), and they decreased over time. These findings suggest that NeoPep S 3ppm has a substantial anti-inflammatory impact and aids in the wound healing process.

Similarly, we determined the level of reactive oxygen species (ROS) on day 7 and day 10, and the inflammation in the wound was observed with a high expression level of reactive oxygen species (ROS). Interestingly, the reactive oxygen species (ROS) levels in the NeoPep S 1ppm and 3 ppm groups were reduced compared with those in the control group over time. The level of reactive oxygen species (ROS) in the NeoPep S 3ppm group at day 10 showed the strongest reduction (Figure 7F-G). Based on these results, we believe that NeoPep S 3ppm could be introduced as a wound healing treatment to remove excess pro-inflammatory mediators, such as nitric oxide (NO) and reactive oxygen species (ROS).

Moreover, to determine the function of nitric oxide (NO) during wound healing and in the regeneration of new tissue in the skin of rat models *in vivo*, purified proteins from the collected tissues at day 7 and day 10 were analyzed to measure the concentration of nitrate (i.e., an end product of nitric oxide generation). High levels of nitric oxide (NO) cause inflammation, later initiating the synthesis of pro-inflammatory mediators and the degradation of extracellular matrix components. As shown in Figure 7H, it was observed that the concentration of nitric oxide (NO) in NeoPep S decreased over time compared with that in the control group. In particular, the concentration of nitric oxide (NO) in the NeoPep S 3ppm group on day 10 was measured at 17.63± 1.41 μM/mg (p=0.016), while it was measured at 18.07± 1.62 μM/mg (p=0.03) in the NeoPep S 1ppm group, and 20.21± 0.81 μM/mg in the control group (Figure 7H).

Figure 7

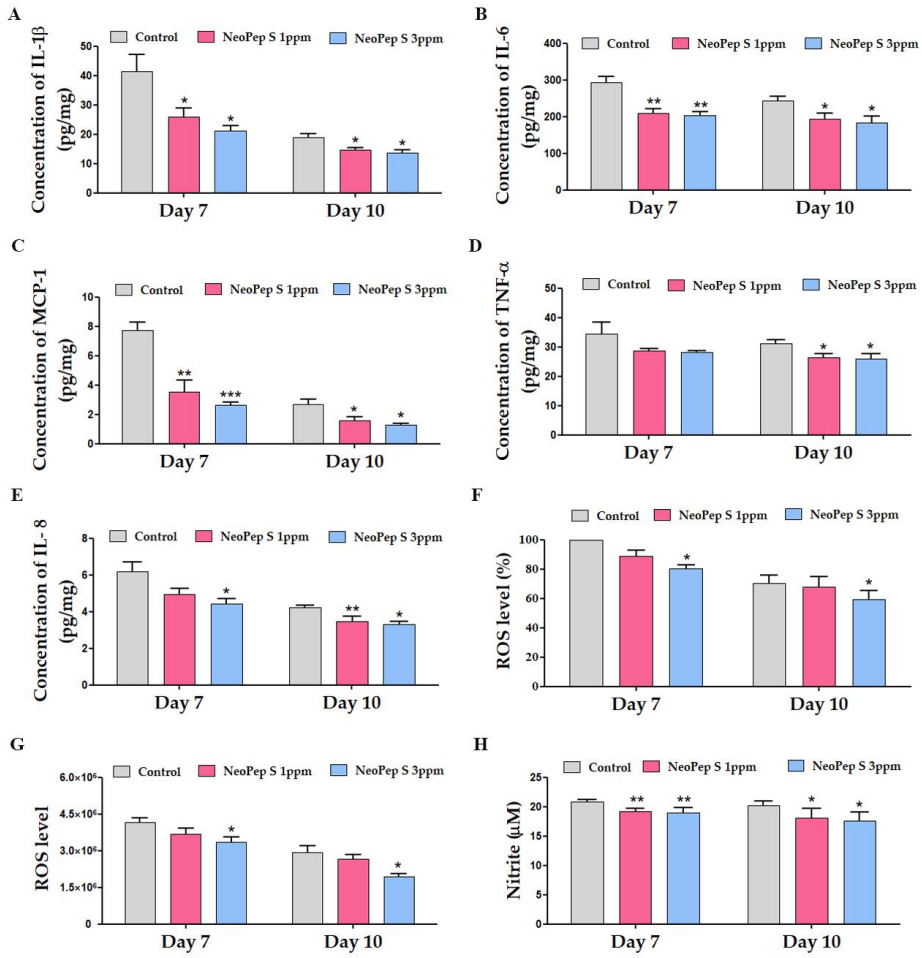
A
Concentration of IL-1β (pg/mg)
Control
NeoPep S 1ppm
NeoPep S 3ppm
Day 7
Day 10
B
Concentration of IL-6 (pg/mg)
C
Concentration of MCP-1 (pg/mg)
D
Concentration of TNF-α (pg/mg)
E
Concentration of IL- 8 (pg/mg)
F
ROS level (%)
G
ROS level
H
Nitrite (μM)

Figure 7. The reduction in inflammatory elements post-wounding. (A-E) The sections of wound tissues confirmed by the enzyme-linked immunosorbent assay (ELISA) showed a down-regulation in the expression of interleukin 1 beta (IL-1β), interleukin 6 (IL-6), interleukin 8 (IL-8), monocyte chemoattractant protein 1 (MCP-1), and tumor necrosis factor alpha (TNF-α) after 7 days and 10 days. (F) Measurement of nitrate and nitrite (NOx) by Griess assay on day 7 and day 10 post-wounding. (G) The levels of reactive oxygen species (ROS) from homogenized wound tissues were investigated and analyzed on the same day of surgery, after 7 days, and after 10 days by DCF-DA assay, and the fluorescent intensity was obtained and calculated using ImageJ software, normalized by the intensity of control. (H) The levels of reactive oxygen species (ROS) are shown by the ratio. ***$p<0.001$, **$p<0.01$, and *$p<0.05$, compared with the control group.

Discussion

The multi-aminoacyl-tRNA synthetase complex is linked to AIMP1 and was identified as a cofactor protein, providing an efficient aminoacyl-tRNA synthesis trafficking pathway for translation (28). Furthermore, aminoacyl tRNA synthetase complex interacting multifunctional protein 1 (AIMP1) levels are higher in damaged skin, and the roles of aminoacyl tRNA synthetase complex interacting multifunctional protein 1 (AIMP1) in the wound healing process (e.g., stimulating re-epithelialization and revascularization, neutralizing lipopolysaccharide (LPS), and performing as immunomodulators) are worth noting (29-35).

The process of wound healing is impacted by a variety of factors. In the present research, we investigated the effects of NeoPep S on the process of wound healing, confirmed as faster re-epithelialization, granulation tissue thickness, increased fibroblasts, elevated collagen deposition, and decreased inflammation. Moreover, NeoPep S can inhibit the inflammatory production of cytokines such as tumor necrosis factor alpha (TNF-α), interleukin 1 beta (IL-1β), monocyte chemoattractant protein 1 (MCP-1), interleukin 6 (IL-6), and interleukin 8 (IL-8) in lipopolysaccharide (LPS)-stimulated RAW 264.7 cells, suggesting that NeoPep S may contribute to the wound healing process via the promotion of fibroblast migration in the wound site.

Wound healing is a complicated process consisting of a series of steps, including hemostasis, inflammation, proliferation, migration, extracellular matrix formation, and remodeling to reconstruct the natural barrier between the body and the external environment (36). A variety of wound-related signaling networks contribute to re-epithelialization, such as nitric oxide, which is mostly produced by macrophages (37), cytokines, and growth factors, including heparin-

binding epidermal growth factor (HB-EGF), fibroblast growth factor (FGF), transforming growth factor (TGF), nerve growth factor (NGF), epidermal growth factor (EGF), platelet-derived growth factor (PDGF), and granulocyte-macrophage colony-stimulating factor (GM-CSF), secreted from many cell types in the wound (38-43). In our *in vivo* study, the formation of re-epithelialization occurred more quickly compared with the control group on days 7 and 10. The addition of NeoPep S promoted the fast formation of the epidermis layer, as well as wound closure. These results may be explained by the enhancing rate of proliferation, migration, and differentiation of keratinocytes in response to NeoPep S.

Macrophages and inflammation are known to play an important role in wound healing through inflammation, proliferation, and remodeling. Inflammation and chronic inflammation are both important stages in wound healing. Shortly after an injury, the innate immune system is activated, triggering a local inflammatory response that initiates the complement cascade and leads to neutrophil infiltration surrounding the wound site, the primary role of which is to prevent infection. Neutrophils phagocytose foreign substances and bacteria in the wound environment, killing them using proteolytic enzymes and oxygen-derived free radical species. However, the long-time gathering of leukocytes will influence the wound healing process. In the current investigation, the wounds treated with NeoPep S demonstrated a reduced level of inflammatory cytokines, such as interleukin 1 beta (IL-1 β), tumor necrosis factor alpha (TNF-α), monocyte chemoattractant protein 1 (MCP-1), interleukin 6 (IL-6), and interleukin 8 (IL-8) (via enzyme-linked immunosorbent assay and the immunofluorescence staining method) compared with those in the control group, as evidenced by the considerably lower neutrophil and macrophage production in the wound bed. In wound healing, the local macrophage population shifts from the pro-inflammatory phenotype (M1 phenotype) to the anti-inflammatory phenotype (M2 phenotype). Macrophages in M1 have the ability to kill off pathogens in wounded tissues that are virally infected,

whereas macrophages in M2 play an important role in the formation of granulation tissue, cell proliferation, and tissue repair (44-46). The polarization of macrophages from M1 to M2 has been reported to help in the process of wound healing and regeneration (47, 48). In our research, treatment of the wounds with NeoPep S promoted the polarization of the macrophages forward to the M2 phenotype. The levels of pro-inflammation cytokines in our *in vivo* research were decreased in the treated wounds in the NeoPep S groups. Moreover, the results of this *in vivo* study demonstrated that NeoPep S suppresses the production of inflammatory cytokine biomarkers, including interleukin 1 beta (IL-1β), tumor necrosis factor alpha (TNF-α), monocyte chemoattractant protein 1 (MCP-1), and interleukin 6 (IL-6), secreted from inflamed RAW 264.7 cells. Therefore, the decrease in inflammation cytokines in the treated wounds in the NeoPep S groups and the inflamed RAW 264.7 cells suggests that NeoPep S contributed to inhibiting the inflammation and improving the wound-healing process observed in this study.

Fibroblasts are crucial in processes such as breaking down the fibrin clot and establishing new extracellular matrix and collagen structures to assist other cells that are needed for efficient wound healing, as well as wound closure (49). Vimentin is expressed in activated fibroblasts and plays an important role in extracellular matrix production, transforming growth factor 1 beta (TGF-1β) slug signaling, collagen accumulation, and the remodeling that occurs during wound healing (50, 51). Recent studies have shown that vimentin knockout mice present systemic defects that are related to the development and wound repair (52, 53). Therefore, the results showed the intensity of vimentin observed on days 7 and 10 using an immunofluorescence (IF) staining (Figure 4A-C). The expression of vimentin in the wounds treated with NeoPep S was higher compared with that in the control group over time. The NeoPep S 3ppm group measured the highest expression during the wound healing process. In our *in vivo* experiment, the results showed a high expression of vimentin similar to that found in previous studies, in which the role of

vimentin in wound healing was discovered (50, 54). Our findings showed that NeoPep S may contribute to the process of wound healing through the expression of vimentin by regulating fibroblast proliferation, collagen accumulation, and epithelial–mesenchymal transition (EMT), all of which influence keratinocyte activation. Furthermore, the process of collagen synthesis plays an important role in each phase of wound healing. Collagen encourages the formation of new collagen in the wound bed by the stimulation of fibroblasts. It contributes to the physical strength and flexibility of the tissue (55). Delayed or extended collagen deposition, on the other hand, can lead to the creation of chronic inflammation of wounds and scars. Therefore, the support of balanced collagen deposition may be beneficial to successful cell therapy (56). As shown in Fig. 2F&G, in the *in vivo* experiment, the synthesis of collagen in the wounds treated with NeoPep S was displayed at a higher expression level than that in the control group. These results show that NeoPep S plays an important part in promoting wound repair.

Recent research from both animal and human studies has recognized that nitric oxide (NO) plays an important role in biological functions. Nitric oxide (NO) has been observed in a variety of wound healing processes, such as inflammation response, cell proliferation, collagen synthesis in wound healing, vasodilatation, angiogenesis, tissue fibroblasts, antimicrobial activity, and immunological responses (57, 58). The key role of nitric oxide (NO) in wound healing has drawn a lot of attention and led to nitric oxide (NO)–based wound healing (59). In our research, the level of nitric oxide (NO) in the wounds treated with NeoPep S was significantly decreased, lower than the level in the control group in both *in vitro* and *in vivo* experiments. This indicates that NeoPep S has an important function in inhibiting the inflammation phase of the wound healing process.

Moreover, reactive oxygen species (ROS) also plays a significant

part in the orchestration of the normal wound healing process. Low reactive oxygen species (ROS) levels have a beneficial impact on wound healing, whereas high reactive oxygen species (ROS) production causes oxidative stress, which can be harmful to wound healing (60). In our study, the level of reactive oxygen species (ROS) generation significantly decreased in the groups treated with NeoPep S compared with that in the control group. This finding suggests that NeoPep S contributes to reducing the level of reactive oxygen species (ROS) to accelerate the pro-inflammatory process.

Conclusion

To conclude, the results of *in vivo* and *in vitro* experiments have confirmed that aminoacyl tRNA synthase complex-interacting multifunctional protein 1 (AIMP1)-derived peptides have the ability to promote the skin wound healing process. We applied a very small amount of the peptide (15 amino acids) as a new generation NeoPep S-a new material that promotes wound healing. Through many careful examinations and strict verifications, NeoPep S showed various activities on inflammatory cells, fibroblasts, and myofibroblasts, which all play important roles in the wound healing process. For RAW 264.7 cells stimulated by lipopolysaccharide (LPS), aminoacyl tRNA synthetase complex interacting 1-derived peptide (Adp) significantly inhibited tumor necrosis factor alpha (TNF-α) expression. The NeoPep S 3ppm dose was the most efficient treatment for rat wound healing in comparison with the 1ppm dose. The findings contribute strong evidence of the safety and effectiveness of using a natural protein derivative in the ingredients of clinical products.

References

1. Martin, P. Wound Healing--Aiming for Perfect Skin Regeneration. Science (80-.). 1997, 276, 75-81, doi:10.1126/science.276.5309.75.
2. Takeo, M.; Lee, W.; Ito, M. Wound Healing and Skin Regeneration. Cold Spring Harb. Perspect. Med. 2015, 5, a023267-a023267, doi:10.1101/cshperspect.a023267.
3. Behm, B.; Babilas, P.; Landthaler, M.; Schreml, S. Cytokines, Chemokines and Growth Factors in Wound Healing. J. Eur. Acad. Dermatology Venereol. 2012, 26, 812-820, doi:10.1111/j.1468-3083.2011.04415.x.
4. Kasuya, A.; Tokura, Y. Attempts to Accelerate Wound Healing. J. Dermatol. Sci. 2014, 76, 169-172, doi:10.1016/j.jdermsci.2014.11.001.
5. Martin, P.; Nunan, R. Cellular and Molecular Mechanisms of Repair in Acute and Chronic Wound Healing. Br. J. Dermatol. 2015, 173, 370-378, doi:10.1111/bjd.13954.
6. Elsaie, M.L. Update on Management of Keloid and Hypertrophic Scars: A Systemic Review. J. Cosmet. Dermatol. 2021, 20, 2729-2738, doi:10.1111/jocd.14310.
7. Leavitt, T.; Hu, M.S.; Marshall, C.D.; Barnes, L.A.; Lorenz, H.P.; Longaker, M.T. Scarless Wound Healing: Finding the Right Cells and Signals. Cell Tissue Res. 2016, 365, 483-493, doi:10.1007/s00441-016-2424-8.
8. Armstrong, D.G.; Boulton, A.J.M.; Bus, S.A. Diabetic Foot Ulcers and Their Recurrence. N. Engl. J. Med. 2017, 376, 2367-2375, doi:10.1056/NEJMra1615439.
9. Han, G.; Ceilley, R. Chronic Wound Healing: A Review of Current Management and Treatments. Adv. Ther. 2017, 34, 599-610, doi:10.1007/s12325-017-0478-y.
10. Comegna, D.; Zannetti, A.; Del Gatto, A.; de Paola, I.; Russo, L.; Di Gaetano, S.; Liguoro, A.; Capasso, D.; Saviano, M.; Zaccaro, L. Chemical Modification for Proteolytic Stabilization of the Selective αv β 3 Integrin RGDechi Peptide: In Vitro and in Vivo Activities on

Malignant Melanoma Cells. J. Med. Chem. 2017, 60, 9874-9884, doi:10.1021/acs.jmedchem.7b01590.
11. Nguyen, T.T.; Ding, D.; Wolter, W.R.; Pérez, R.L.; Champion, M.M.; Mahasenan, K. V.; Hesek, D.; Lee, M.; Schroeder, V.A.; Jones, J.I.; et al. Validation of Matrix Metalloproteinase-9 (MMP-9) as a Novel Target for Treatment of Diabetic Foot Ulcers in Humans and Discovery of a Potent and Selective Small-Molecule MMP-9 Inhibitor That Accelerates Healing. J. Med. Chem. 2018, 61, 8825-8837, doi:10.1021/acs.jmedchem.8b01005.
12. Park, S.-R.; Kim, J.-W.; Jun, H.-S.; Roh, J.Y.; Lee, H.-Y.; Hong, I.-S. Stem Cell Secretome and Its Effect on Cellular Mechanisms Relevant to Wound Healing. Mol. Ther. 2018, 26, 606-617, doi:10.1016/j.ymthe.2017.09.023.
13. Dinh, T.; Braunagel, S.; Rosenblum, B.I. Growth Factors in Wound Healing. Clin. Podiatr. Med. Surg. 2015, 32, 109-119, doi:10.1016/j.cpm.2014.09.010.
14. Maver, T.; Maver, U.; Stana Kleinschek, K.; Smrke, D.M.; Kreft, S. A Review of Herbal Medicines in Wound Healing. Int. J. Dermatol. 2015, 54, 740-751, doi:10.1111/ijd.12766.
15. Lordani, T.V.A.; de Lara, C.E.; Ferreira, F.B.P.; de Souza Terron Monich, M.; Mesquita da Silva, C.; Felicetti Lordani, C.R.; Giacomini Bueno, F.; Vieira Teixeira, J.J.; Lonardoni, M.V.C. Therapeutic Effects of Medicinal Plants on Cutaneous Wound Healing in Humans: A Systematic Review. Mediators Inflamm. 2018, 2018, 1-12, doi:10.1155/2018/7354250.
16. de la Torre, B.G.; Albericio, F. Peptide Therapeutics 2.0. Molecules 2020, 25, 2293, doi:10.3390/molecules25102293.
17. de la Torre, B.G.; Albericio, F. The Pharmaceutical Industry in 2019. An Analysis of FDA Drug Approvals from the Perspective of Molecules. Molecules 2020, 25, 745, doi:10.3390/molecules25030745.
18. Kaspar, A.A.; Reichert, J.M. Future Directions for Peptide Therapeutics Development. Drug Discov. Today 2013, 18, 807-817, doi:10.1016/j.drudis.2013.05.011.
19. Fosgerau, K.; Hoffmann, T. Peptide Therapeutics: Current Status and Future Directions. Drug Discov. Today 2015, 20, 122-128,

doi:10.1016/j.drudis.2014.10.003.
20. Demori, I.; Rashed, Z. El; Corradino, V.; Catalano, A.; Rovegno, L.; Queirolo, L.; Salvidio, S.; Biggi, E.; Zanotti-Russo, M.; Canesi, L.; et al. Peptides for Skin Protection and Healing in Amphibians. Molecules 2019, 24, 347, doi:10.3390/molecules24020347.
21. Neenan, T.X.; Burrier, R.E.; Kim, S. Biocon's Target Factory. Nat. Biotechnol. 2018, 36, 791-797, doi:10.1038/nbt.4242.
22. Hong, S.H.; Cho, J.G.; Yoon, K.J.; Lim, D.-S.; Kim, C.H.; Lee, S.-W.; Park, S.G. The Antibody Atliximab Attenuates Collagen-Induced Arthritis by Neutralizing AIMP1, an Inflammatory Cytokine That Enhances Osteoclastogenesis. Biomaterials 2015, 44, 45-54, doi:10.1016/j.biomaterials.2014.12.017.
23. Han, J.M.; Kwon, N.H.; Lee, J.Y.; Jeong, S.J.; Jung, H.J.; Kim, H.R.; Li, Z.; Kim, S. Identification of Gp96 as a Novel Target for Treatment of Autoimmune Disease in Mice. PLoS One 2010, 5, e9792, doi:10.1371/journal.pone.0009792.
24. Kwon, N.H.; Fox, P.L.; Kim, S. Aminoacyl-TRNA Synthetases as Therapeutic Targets. Nat. Rev. Drug Discov. 2019, 18, 629-650, doi:10.1038/s41573-019-0026-3.
25. Park, S.G.; Choi, E.-C.; Kim, S. Aminoacyl-TRNA Synthetase-Interacting Multifunctional Proteins (AIMPs): A Triad for Cellular Homeostasis. IUBMB Life 2010, NA-NA, doi:10.1002/iub.324.
26. Kim, J.; Kang, S.; Kwon, H.; Moon, H.; Park, M.C. Dual Functional Bioactive - peptide, <scp>AIMP</Scp> 1 - derived Peptide (AdP), for Anti - aging. J. Cosmet. Dermatol. 2019, 18, 251-257, doi:10.1111/jocd.12671.
27. Lee, J.-J.; Han, Y.-M.; Kwon, T.-W.; Kim, D.; Lee, H.; Jung, W.; Kim, J.; Kang, S.; Kim, S.; Cho, C.-W.; et al. Functional Fragments of AIMP1-Derived Peptide (AdP) and Optimized Hydrosol for Their Topical Deposition by Box-Behnken Design. Molecules 2019, 24, 1967, doi:10.3390/molecules24101967.
28. Hong, H.-J.; Lim, H.X.; Song, J.H.; Lee, A.; Kim, E.; Cho, D.; Cohen, E.P.; Kim, T.S. Aminoacyl-TRNA Synthetase-Interacting Multifunctional Protein 1 Suppresses Tumor Growth in Breast Cancer-Bearing Mice by Negatively Regulating Myeloid-Derived

Suppressor Cell Functions. Cancer Immunol. Immunother. 2016, 65, 61-72, doi:10.1007/s00262-015-1777-2.
29. Hancock, R.E.W.; Sahl, H.-G. Antimicrobial and Host-Defense Peptides as New Anti-Infective Therapeutic Strategies. Nat. Biotechnol. 2006, 24, 1551-1557, doi:10.1038/nbt1267.
30. Rosenfeld, Y.; Papo, N.; Shai, Y. Endotoxin (Lipopolysaccharide) Neutralization by Innate Immunity Host-Defense Peptides. J. Biol. Chem. 2006, 281, 1636-1643, doi:10.1074/jbc.M504327200.
31. Mookherjee, N.; Brown, K.L.; Bowdish, D.M.E.; Doria, S.; Falsafi, R.; Hokamp, K.; Roche, F.M.; Mu, R.; Doho, G.H.; Pistolic, J.; et al. Modulation of the TLR-Mediated Inflammatory Response by the Endogenous Human Host Defense Peptide LL-37. J. Immunol. 2006, 176, 2455-2464, doi:10.4049/jimmunol.176.4.2455.
32. Tjabringa, G.S.; Aarbiou, J.; Ninaber, D.K.; Drijfhout, J.W.; Sørensen, O.E.; Borregaard, N.; Rabe, K.F.; Hiemstra, P.S. The Antimicrobial Peptide LL-37 Activates Innate Immunity at the Airway Epithelial Surface by Transactivation of the Epidermal Growth Factor Receptor. J. Immunol. 2003, 171, 6690-6696, doi:10.4049/jimmunol.171.12.6690.
33. Akiyama, T.; Niyonsaba, F.; Kiatsurayanon, C.; Nguyen, T.T.; Ushio, H.; Fujimura, T.; Ueno, T.; Okumura, K.; Ogawa, H.; Ikeda, S. The Human Cathelicidin LL-37 Host Defense Peptide Upregulates Tight Junction-Related Proteins and Increases Human Epidermal Keratinocyte Barrier Function. J. Innate Immun. 2014, 6, 739-753, doi:10.1159/000362789.
34. Carretero, M.; Escámez, M.J.; García, M.; Duarte, B.; Holguín, A.; Retamosa, L.; Jorcano, J.L.; Río, M. del; Larcher, F. In Vitro and In Vivo Wound Healing-Promoting Activities of Human Cathelicidin LL-37. J. Invest. Dermatol. 2008, 128, 223-236, doi:10.1038/sj.jid.5701043.
35. Ramos, R.; Silva, J.P.; Rodrigues, A.C.; Costa, R.; Guardão, L.; Schmitt, F.; Soares, R.; Vilanova, M.; Domingues, L.; Gama, M. Wound Healing Activity of the Human Antimicrobial Peptide LL37. Peptides 2011, 32, 1469-1476, doi:10.1016/j.peptides.2011.06.005.
36. Tottoli, E.M.; Dorati, R.; Genta, I.; Chiesa, E.; Pisani, S.; Conti, B.

Skin Wound Healing Process and New Emerging Technologies for Skin Wound Care and Regeneration. Pharmaceutics 2020, 12, 735, doi:10.3390/pharmaceutics12080735.
37. Witte, M.B.; Barbul, A. Role of Nitric Oxide in Wound Repair. Am. J. Surg. 2002, 183, 406-412, doi:10.1016/S0002-9610(02)00815-2.
38. Barrientos, S.; Stojadinovic, O.; Golinko, M.S.; Brem, H.; Tomic-Canic, M. PERSPECTIVE ARTICLE: Growth Factors and Cytokines in Wound Healing. Wound Repair Regen. 2008, 16, 585-601, doi:10.1111/j.1524-475X.2008.00410.x.
39. Pastar, I.; Stojadinovic, O.; Yin, N.C.; Ramirez, H.; Nusbaum, A.G.; Sawaya, A.; Patel, S.B.; Khalid, L.; Isseroff, R.R.; Tomic-Canic, M. Epithelialization in Wound Healing: A Comprehensive Review. Adv. Wound Care 2014, 3, 445-464, doi:10.1089/wound.2013.0473.
40. WERNER, S.; GROSE, R. Regulation of Wound Healing by Growth Factors and Cytokines. Physiol. Rev. 2003, 83, 835-870, doi:10.1152/physrev.2003.83.3.835.
41. Raja, R. Wound Re-Epithelialization: Modulating Kerationcyte Migration in Wound Healing. Front. Biosci. 2007, 12, 2849, doi:10.2741/2277.
42. Grzela, T.; Krejner, A.; Litwiniuk, M. Matrix Metalloproteinases in the Wound Microenvironment: Therapeutic Perspectives. Chronic Wound Care Manag. Res. 2016, 29, doi:10.2147/CWCMR.S73819.
43. Michopoulou, A.; Rousselle, P. How Do Epidermal Matrix Metalloproteinases Support Re-Epithelialization during Skin Healing? Eur. J. Dermatology 2015, 25, 33-42, doi:10.1684/ejd.2015.2553.
44. Hesketh, M.; Sahin, K.B.; West, Z.E.; Murray, R.Z. Macrophage Phenotypes Regulate Scar Formation and Chronic Wound Healing. Int. J. Mol. Sci. 2017, 18, 1545, doi:10.3390/ijms18071545.
45. Italiani, P.; Boraschi, D. From Monocytes to M1/M2 Macrophages: Phenotypical vs. Functional Differentiation. Front. Immunol. 2014, 5, doi:10.3389/fimmu.2014.00514.
46. Kotwal, G.J.; Chien, S. Macrophage Differentiation in Normal and Accelerated Wound Healing. In; 2017; pp. 353-364.
47. Ferrante, C.J.; Leibovich, S.J. Regulation of Macrophage Polarization and Wound Healing. Adv. Wound Care 2012, 1, 10-16,

doi:10.1089/wound.2011.0307.
48. Kim, S.Y.; Nair, M.G. Macrophages in Wound Healing: Activation and Plasticity. Immunol. Cell Biol. 2019, 97, 258-267, doi:10.1111/imcb.12236.
49. P., B. Wound Healing and the Role of Fibroblasts. J. Wound Care 2013, 22, 407-412, doi:10.12968/jowc.2013.22.8.407.
50. Cheng, F.; Shen, Y.; Mohanasundaram, P.; Lindström, M.; Ivaska, J.; Ny, T.; Eriksson, J.E. Vimentin Coordinates Fibroblast Proliferation and Keratinocyte Differentiation in Wound Healing via TGF-β-Slug Signaling. Proc. Natl. Acad. Sci. 2016, 113, E4320-E4327, doi:10.1073/pnas.1519197113.
51. Nomura, S. Identification, Friend or Foe: Vimentin and α-Smooth Muscle Actin in Cancer-Associated Fibroblasts. Ann. Surg. Oncol. 2019, 26, 4191-4192, doi:10.1245/s10434-019-07894-8.
52. Battaglia, R.A.; Delic, S.; Herrmann, H.; Snider, N.T. Vimentin on the Move: New Developments in Cell Migration. F1000Research 2018, 7, 1796, doi:10.12688/f1000research.15967.1.
53. Eckes, B.; Colucci-Guyon, E.; Smola, H.; Nodder, S.; Babinet, C.; Krieg, T.; Martin, P. Impaired Wound Healing in Embryonic and Adult Mice Lacking Vimentin. J. Cell Sci. 2000, 113, 2455-2462, doi:10.1242/jcs.113.13.2455.
54. Parvanian, S.; Zha, H.; Su, D.; Xi, L.; Jiu, Y.; Chen, H.; Eriksson, J.E.; Cheng, F. Exosomal Vimentin from Adipocyte Progenitors Protects Fibroblasts against Osmotic Stress and Inhibits Apoptosis to Enhance Wound Healing. Int. J. Mol. Sci. 2021, 22, 4678, doi:10.3390/ijms22094678.
55. Mathew-Steiner, S.S.; Roy, S.; Sen, C.K. Collagen in Wound Healing. Bioengineering 2021, 8, 63, doi:10.3390/bioengineering8050063.
56. Xue, M.; Jackson, C.J. Extracellular Matrix Reorganization During Wound Healing and Its Impact on Abnormal Scarring. Adv. Wound Care 2015, 4, 119-136, doi:10.1089/wound.2013.0485.
57. Childress, B.B.; Stechmiller, J.K. Role of Nitric Oxide in Wound Healing. Biol. Res. Nurs. 2002, 4, 5-15, doi:10.1177/1099800402004001002.

58. Wu, M.; Lu, Z.; Wu, K.; Nam, C.; Zhang, L.; Guo, J. Recent Advances in the Development of Nitric Oxide-Releasing Biomaterials and Their Application Potentials in Chronic Wound Healing. J. Mater. Chem. B 2021, 9, 7063-7075, doi:10.1039/D1TB00847A.
59. Kitano, T.; Yamada, H.; Kida, M.; Okada, Y.; Saika, S.; Yoshida, M. Impaired Healing of a Cutaneous Wound in an Inducible Nitric Oxide Synthase-Knockout Mouse. Dermatol. Res. Pract. 2017, 2017, 1-11, doi:10.1155/2017/2184040.
60. Dunnill, C.; Patton, T.; Brennan, J.; Barrett, J.; Dryden, M.; Cooke, J.; Leaper, D.; Georgopoulos, N.T. Reactive Oxygen Species (ROS) and Wound Healing: The Functional Role of ROS and Emerging ROS-Modulating Technologies for Augmentation of the Healing Process. Int. Wound J. 2017, 14, 89-96, doi:10.1111/iwj.12557.

Abstract in Korean

피부는 기계적 손상, 미생물 감염, 자외선 및 극한 온도로부터 신체를 보호하는 데 중요한 역할을 한다. 본 연구는 NeoPep S 및 다른 상처 치유 제품들의 피부 손상 및 복구 효능에 중점을 두어 진행되었다. 현재 시장에 나와 있는 상처치유 약물은 증가하는 의료 수요를 충족시키기에는 충분하지 않으며 여전히 해결해야 할 난제들에 직면해 있는 상황이다. 본 연구는 NeoPep S 의 상처 회복과 피부 재생 촉진을 효율적으로 조절할 수 있는지 알아보도록 설계되었다. 이 연구에서 우리는 새로운 AIMP1 유래 펩타이드(AdP)인 NeoPep S를 두 가지 용량 유형(1ppm 및 3ppm)으로 투여하고 쥐 모델에서 피부 상처 복구에 미치는 영향을 결정했습니다. 면역형광(IF) 염색 및 ELISA를 사용하여 세포 증식 및 염증 반응을 평가하였다. 우리의 결과는 NeoPep S 1ppm보다 NeoPep S 3ppm으로 치료할 때 상처 봉합에서 더 빠르고 만족스러운 효능을 보여주었다. AIMP1 단백질에서 유래한 3ppm 펩타이드는 상처와 조화롭게 상호작용하여 재상피화 및 콜라겐 재생을 촉진할 뿐만 아니라 종양괴사인자 알파(TNF-α), 인터류킨 6(IL-6), 인터류킨 8(IL-8)과 같은 여러 유형의 사이토카인 및 케모카인의 하향 조절을 촉진하였다. 더욱이, 인터류킨 1 베타(IL-1β), 단세포 화학유인제 단백질 1(MCP-1), F4/80, 전환성장인자 베타 1(TGF-β1) 및 전환성장인자 베타 3(TGF-β3) 조절뿐만 아니라 아질산염 및 반응성 산소 종 소거에 의해 섬유아세포 증식, 이동 및 분화를 촉진하는 것으로 입증되었다. 결론적으로 본 연구를 통해 새로운 펩타이드 NeoPep S은 상처 치유에 높은 효과와 안전성을 가지고 있으며 가까운 장래에 선도적인 상처 관리 제품 중 하나가 될 큰 가능성을 보여주었다.